Investigation of the effect of consolidation on cement flow behaviour

Turki, D., Saidani, M., Belarbi, E-H. & Fatah, N.

Original citation & hyperlink:
Turki, D, Saidani, M, Belarbi, E-H & Fatah, N 2018, 'Investigation of the effect of consolidation on cement flow behaviour' Advances in Cement Research, vol. (In-press), ACR-D-17-00178R2, pp. (In-press).
https://dx.doi.org/10.1680/jadcr.17.00178

DOI 10.1680/jadcr.17.00178
ISSN 0951-7197
ESSN 1751-7605

Publisher: Thomas Telford (ICE Publishing)

Main Text

Research Article
Paper ACR-D-17-00178
Received 05/10/2017; Revised 13/11/2018
Number of words 3799, number of Figures 10

Investigation of the effect of consolidation on cement flow behaviour

Djamel TURKI, Dr.

Univ-Tiaret, Laboratoire de Génie électrique et des plasmas, Tiaret, Algeria.

Messaoud SAIDANI, Dr.

Coventry University, Faculty of Engineering and Computing, Coventry, UK.

El-habib BELARBI, Pr.

Univ-Tiaret, Laboratoire Synthèse et Catalyse, Tiaret, Algeria.

Nouria FATAH, Pr.

Unité de Catalyse et Chimie du Solide, UMR CNRS 8181, ENSC Lille, France.

Correspondence address:

Dr. Djamel TURKI
Université Ibn-Khaldoun deTiaret,
Laboratoire de Génie électrique et des plasmas,
BP 78, 14000 Tiaret,
Algeria
Tel.:213664119700
Fax: 21346410225
e-mail: turkidjamel@yahoo.fr

Abstract

One of the main problems affecting the flow of cement bulk powder is the formation of cohesive arching at the outlet of the hopper, causing blocking of the silo opening and bridge formation. A simple concept is established which outlines these complications. In this context, the interactions of particles lead to a high degree of consolidation of the cement powder and an increase of adhesion force due to the small size and the large surface area of the cement particles. The results from the consolidation test and the flow properties (cohesion) show that the cement powder flow is mainly controlled by internal forces (Van der Waals and adhesion forces) and external forces. These forces have a direct influence on the powder structure, leading to a variable packing behaviour.

Since the problem is due mainly to the interparticle forces, before storage of the cement powder in silo, the powder should be fluidised with air at high velocity to disintegrate the cohesive structure and to overcome over this undesirable property of cement flow.

Keywords: Compressive strength; Modeling; Rheological/rheological properties; Stress; Set-packing.

Notation

F_N	Normal force
F_{VdW}	Van der Waals force
F_s	Adhesion force
A	Hamaker constant
D	Reduced diameter
z	Distance between the two particles
s_c	Contact surface ($s_c = \pi r^2$)
r	Radius of the contact surface
F_s	Adhesion force
R	Particle radius
K	Reduced Young's modulus
σ	External stress
d_p	Average particle diameter
n	Coordination number
$F_{ex.}$	External force
S	Cell surface
M	Mass of the powder in the cell
h	Height of the packed bed of particles
$(1\text{-}\varepsilon)$	Solid fraction
ρ_p	Particle density
τ_c	Cohesion
σ_1	Maximum stress
σ_c	Compressive resistance
Ni	Number of particles in class i
d_i	Average diameter of the particles in class i
FF_c	Flow property.

1. Introduction

Several cement plants deal with bulk flow problems that have a detrimental impact on production efficiency, as described by Maynard (2004). Most of the methods used for measuring the flowability of cement make use of some concepts developed in powder mechanics as shown by Maynard (2004). The cement powder flow is mainly controlled by internal and external forces. These forces are the main cause for agglomerating the cement particles in concrete and of resulting of poor flow properties, as discussed by Flatt (2004).

The physical properties of cement powder are directly related to the conception of appropriate and efficient storage equipment as shown by Ganesan et al. (2008). The consolidation and porosity of the solid structure are linked to the understanding of the cement powder flow behaviour, as reported by Leturia et al. (2014). Holdich (2002) stated that the effect that the solid fraction has on flowability powder is probably the most interesting part of the investigation. The powder structure porosity is mainly related to the bulk density which is the combined density of the powder and the void space as shown by Holdich (2002).

The complexity of the cement powder structure requires an examination of the powder behaviour, in particular the particles interaction and pore description. The small size and the large surface area of the cement particles lead to the formation of agglomerates and change the porosity of the solid structure that may be reduced by polymeric dispersants addition, as stated by Uchikawa et al. (1997), Ramachandran et al. (1998) and Aïtcin et al. (1994). The consolidation of the powder would reduce the void of the structure and hence increases the effectiveness and toughness of the material, as described by Li and Kwan (2014). The packed density of the cement powder is a basic aspect governing the effectiveness of concrete as confirmed by Li and Kwan (2014). The adhesion forces can incite efficiency reduction in the industrial processes, as described by Siegel et al. (1963). Flatt (2004) showed that the flowability of a powder structure is related to the adhesive forces between individual particles.

Understanding the behaviour of adhesion interactions between particles and surfaces can contribute to the understanding of the cement powder flow. The different forces involved have to be considered under consolidation namely the Van der Waals, the adhesive and external forces, as was showed by Turki and Fatah (2010). In this context, Flatt (2004) showed that it is essential to evaluate the magnitude of the attractive interparticle forces.

The aim of this research is to present a simple model that takes into account the interparticle forces and the variation of porosity of cement powder bed under external stress (consolidation). That is used to explain the cohesion and the other explicit macroscopic properties of the cement powder flow. The adhesive forces of the cement powder structure are examined and related to the flow obstruction in a silo.

2. Models related to the interparticle forces

Forsyth et al. (2002) elucidated that the interparticle forces between particles of group C Geldart (1973) classification are significant compared to the inertial and gravitational forces, causing poor particle flowability. The adhesion forces would increase with compaction. Schulze (2008) and Tomas (2007) reported that the adhesive forces acting between the particles increase when the particles are constrained to each other by external forces, showing that significant interactions between particles occur, leading to plastic deformation of the particles in the contact region. In this situation Schulze (2008) and Tomas (2007) described that the powder cement flow is principally related to the forces or stresses formerly acting on the powder structure. These forces comprise the consolidation stress exerted on the powder structure, with resulting increase of the adhesion force and hence forming a more compact powder. These concepts rely on interparticle forces estimations that are subject to the appropriate models and assumptions made by Schulze (2008), Tomas (2007).

The behaviour of cohesive powders is outlined principally by the contact of external forces acting on the surface of particles and the cohesion due to the interparticle forces (Van der Waals and adhesion forces). Molerus (1975) assumed that during consolidation, the total normal force due to external force is in equilibrium with other forces.

$$F_N = F_{VdW} + F_s$$

1.

The Van der Waals force between particles is the main parameter that dominates the powder cohesion as stated by Rumpf (1962), and controls the adhesion between fine particles and, in turn, affects the bulk behaviour of powder. Li et al. (2006) and Tomas (2007) stated that the influence of particle adhesion is defined by surface forces i.e. Van der Waals forces. However, under external stress, particles may deform when in contact with each other as reported by Castellanos (2005).

The London-Van der Waals attractive force at solid interface occurring as a result of changing dipoles at the atomic level were integrated by Hamaker (1937) to estimate the attraction between molecules. The Hamaker theory (1937) is used to estimate the Van der Waals force. This force is considered only when the particle surfaces are closer as confirmed by London (1937). An improved model suggested by Langbein (1969) and Götzinger and Peukert (2003) mainly considers the surface properties of particles.

The Van der Waals force is deduced from the energy interaction between two particles given by Xie (1997) as:

$$F_{VdW} = \frac{AD}{12z^2}\left[1+\frac{s_c}{\pi Dz}\right]$$

2.

Johnson et al. (1971) showed that r is given as:

$$r^3 = \frac{3F_s R}{K}$$

3.

The normal force as outlined by Equation (1) can be written as:

$$F_N = \frac{AR}{12z^2}\left[1+\frac{s_c}{\pi Rz}\right]+F_s = \frac{AR}{12z^2}\left[1+\frac{3^{2/3}F_s^{2/3}}{R^{1/3}z\,K^{2/3}}\right]+F_s$$

4.

The adhesive force F_s in the contact of packed particles resulting from the application of external stress σ is given by Rumph (1962) as:

$$F_s = \frac{\sigma\pi d_p^2}{(1-\varepsilon)n}$$

5.

According to Nakagaki and Sunada (1968), the coordination number n is given by:

$$n = 1.61\varepsilon^{-1.48} \quad (\varepsilon \le 0.82)$$

6.

The adhesive force is expressed with the particle diameter, therefore for different particle size distributions, theoretically, the adhesive force would remain the same if the particle-particle interactions have the same magnitude of interaction in the sample of analysis, but in fact the particle size distribution depends on the arrangement of the particles (particles interactions especially for fine powders categorized in the class C of Geldart (1973) classification. It is complex to calculate the adhesion force for each particle in the particle size distribution. To make the problem less complex, we consider the average diameter (applicable only for a uniform distribution) and assuming that the contact is between two particles that have the same average diameter.

3. Experimental procedure

3.1 Material and methods

The powder used in this work is the ordinary Portland cement (OPC) of class CEM II/A-L 42.5 N.

The relative content of oxide in the cement powder is determined with the use of an energy dispersive micro-XRay Fluorescence spectrometer M4 TORNADO (Bruker). This instrument is equipped with 2 anodes a Rhodium X-ray tube 50 kV/600 mA (30 W) and a Tungsten X-Ray tube 50 kV/700 mA (35 W). For sample characterization, the X-rays Rhodium with a polycapillary lens enabling excitation of an area of 200 µm was used. The measurement was done under vacuum (20 mbar). The elements, that can be measured by this instrument unit range from sodium *Na* to uranium *U*. Quantitative analysis was done using fundamental parameter (FP) (standardless). As elements are present in stoichiometric compounds, its formula was used for quantification of the weight percent of each element.

For each sample 36 points (of 200 μm) were analysed, the results are showed as elemental and stoichiometric analysis (based on Formula of the oxide). For each sample, the mean value and standard deviation are presented in Table 1a.

The physical characteristics of the cement powder according to the Algerian Norms (NA442), which is equivalent to the European Standard EN 197-1:2011, and that used in this study are indicated in Table 1b.

3.1.1 X-ray diffraction characterization

X-ray diffraction measurements of the studied cement were performed on a Rigaku Miniflex-600 using SC-70 detector. The powder diffraction patterns of the cement were recorded using Bragg–Brentano geometry and Cu-Kα radiation (λ = 1.5406 Å) in the range of 3°–80° 2θ. A scan rate of 5°/min was used. The Rigaku PDXL 2 software was used to analyze the diffraction pattern.

3. 1.2 Scanning Electron Microscope

The microscopic morphology of the Alite particles was examined by using a SEM Hitachi SN-3400.

3.2 Consolidation Test

To estimate the extent of cohesiveness of the cement powder, a consolidation test was carried out to examine the variation of the powder volume and the reduction of the porosity tendency under normal stress.

The consolidation test is reported in a previous article by Turki et al (2015) and was carried out on the cement powder to analyse the variation of the powder volume and the reduction of the porosity under normal stress.

This test is not a measurement of flowability but is associated with various environmental processes, such as storage in hoppers as reported by Leturia et al. (2014). Figure 1 shows the consolidation test as described by Turki et al. (2015). The external stress is written as:

$$\sigma = \frac{F_{ex.}}{S}$$

7.

Consequently, the difference of the solid fraction (*1-ε*) is considered and correlated to the external stress *σ* by the relationship:

$$1\text{-}\varepsilon = \frac{M}{\rho_p Sh}$$

8.

3.3 Shear Cell

The flow of the powder depends on its consolidation. The effect of consolidation stress on the powder is dependent of the packing and rearrangement of the particles. Accordingly, it is fundamental to assess the flowability of the powder according to the consolidation condition as stated by Diederich et al. (2012). The flowability and cohesion of powder were presented in a previous research, Turki et al. (2015). The measurements of the flowability and cohesion of powders were made with the shear cell of Schulze (1995) as illustrated in Figure 2.

4. Results and discussion

4.1 Cement characterization

The Figure 3 shows the diffraction patterns obtained by the X-ray diffraction characterization.

The content of the cement is estimated by quantitative analysis of the diffraction patterns Figure 3, based on the reference intensity ratio (RIR) method integrated in the PDXL 2. Software. The different phases present in our sample are presented in Table 2.

The X-ray diffraction measurements investigation indicates that the principal silicate phases existing in all the samples are Alite, tricalcium silicate Ca_3O_5Si.

To observe the microscopic morphology of the Alite particles, the cement powder was analyzed by scanning electron microscope using a SEM Hitachi SN-3400. Figure 4 shows the polymorphism of the Alite particles and the surfaces geometry.

The polymorphism of the Alite particles as shown by Courtial et al. (2003) might have a great impact on the cement powder cohesion. Subsequently, the particle surfaces are closer which enhance the Van der Waals forces interaction Hamaker (1937). As illustrated by SEM photos in Figure 4, surface geometry has an important effect on the interaction between particles. This gives an insight towards modelling these interactions using surface-geometry based models.

4.2 Powder size distribution

The powder size distribution illustrated in Figure 5 was measured with a laser light-scattering instrument (Beckman-Coulter, LS230).

The average diameter of the cement powder was calculated in accordance to the Sauter diameter definition “surface volume”. Explicitly, the average diameter is calculated according to the diameter definition “Surface-Volume” or Sauter diameter as

$$d_p = \frac{\Sigma N_i d_i^3}{\Sigma N_i d_i^2}$$

9.

Where N_i is the number of particles in class i and d_i is the average diameter of the particle in this class.

The average diameter was given by the laser light-scattering instrument (Beckman-Coulter, LS230), using the Algorithm to compute the Sauter diameter from a large set of data, giving an average diameter of 4.6 μm.

The particle density ρ_p was measured with a helium pycnometer (Micromeritics, AccuPyc 1330) giving a density of 3577 kg/m^3. Taking into account the particle density and the average size of the cement powder, the powder can be categorized under group C of the Geldart (1973) classification.

4.3 Powder flow and consolidation

The yield locus and the variation in solid fraction according to the normal stress of the cement powder are illustrated in Figure 6 and Figure 7, respectively. As enlightened by Turki et al. (2015).

The results of flowability and cohesion of powder were presented in a previous research, Turki et al. (2015). Figure 6 indicates that the cohesion τ_c=578 Pa. From the yield locus, the maximum stress σ_1=5370 Pa and the compressive resistance σ_c=2169 Pa. The parameter FF_c is defined as the ratio between σ_1 and σ_c that defines the flow property. FF_c was found to be 2.48, resulting that the cement powder is classified as cohesive, difficult flow.

During consolidation, the cement powder structure is uniform and formed by a number of particles in contact. The variation of the solid fraction is mainly due to the interparticle forces and tends to attain a linear regime, Figure 7.

From the consolidation test and using the models developed in Equation (4) and Equation (5). With a Hamaker constant *A* of Ordinary Portland Cement (OPC) as 1.72×10^{-20} J. given by Lomboy et al. (2011) and the cement particle diameter of 4.6μm. The distance between particle surfaces *z* is taken as 4×10^{-10} m, according to Krupp (1967). The reduced Young's modulus is given by Boumiz et al. (1997) as 117.6 GPa.

The variation of the adhesion force F_s to the normal force F_N obtained from Equation (4) is illustrated in Figure 8. The adhesive force starts increasing linearly with the normal force, showing that at initial stage important air diffusion occurs within the powder structure, with the contact number between particles arising from the adhesion forces. Then the particles start to be set in a compact arrangement. Subsequently, a strong cohesion between particles occurs, leading to the formation of an important number of agglomerates. This confirms that the behaviour of cement powder under consolidation is controlled by the internal forces.

For higher values of adhesion force, the transition region is attained resulting in an increase of solid fraction and attainment of a linear regime. The load is extended on the solid structure. Thus, there is consolidation of the packed bed of powder. Consequently, the cement powder flow is mainly affected by the adhesion forces and internal forces due to the time consolidation of cement in the silo as stated by Schulze (1995). As the adhesion force increases, the impact of the Van der Waals forces on the behaviour becomes considerable in forming a large number of agglomerates as illustrated in Figure 9 using Equation (2). Confirming that the interaction between particles is important and this validates the results of the shear test as stated by Turki et al. (2015). Consequently, taking into account the flow of the cement powder in a silo without consolidation, the powder is subjected to its weight that plays the role of the adhesive forces, involving an increase in the Van der Waals forces, hence causing a larger cohesion between particles and then generating a clogging at the silo outlet.

This behaviour is confirmed in Figure 10, showing the evolution of the solid fraction according to the adhesion force where the first part of the graph increases linearly with a straight up development, showing an enhancement in the solid fraction by evacuating the air in the powder structure.

Figure 10 is deduced from the consolidation test resulting in determining the solid fraction (1-ε) and a combination of the adhesion force F_s given by the equation of Rumph (1962), equation 5. Then, the structure is formed of a partial uniform powder. This behaviour is expected to reflect a disintegration of the agglomerates and an increase of the contact surfaces between the particles. The solid fraction-adhesion force curve shows a large upward change of the solid fraction to give a more stable solid structure.

This research revealed that the consolidation test and the flow properties highlight that the cohesion of cement powder is controlled by internal forces and external forces. Throughout the exertion of external forces, different interactions take place in the powder structure. Furthermore, it is interesting to find the relationship between the impact of the Van der Waals forces acting as an isolated interaction to the adhesive forces, that highlights the powders' particle to agglomerate under the action of the powder weight and, therefore, stopping the free flowing of the cement powder.

Similarly, Figure 8 and Figure 10 show the variation of the adhesive and Van der Waals forces with the normal force and the solid fraction respectively, resulting from the consolidation test and using the force equilibrium model of Molerus (1975). These figures highlight the considerable role of the internal forces in forming cohesive arching at the outlet of the hopper.

The deformation of the contact surfaces between the particles facilitates the increase of the Van der Waals forces, resulting in an expansion of the contact region, as confirmed by Krupp (1967). This deformation is due to the adhesion forces; ensuing an enhancement of particles cohesion primarily due to consolidation.

5. Conclusion

Understanding the relationship between the cement powder flow and the adhesion forces is the way to overcome the obstruction for the cement powder flow. Cement powder flow was investigated and quantified by using various techniques such as shear stress and consolidation.

The interparticle forces are at the origin of the formation of arches at the base of the silo mainly due to an increase in adhesion forces. The cement powder has a tendency to consolidate to form a more compact structure and therefore hinder the flow.

The results from the consolidation test and the flow properties (cohesion) show that the cement powder flow is mainly controlled by internal forces (Van der Waals and adhesion forces) and external forces.

As these results confirm the blocking of the silo opening a further research would be carried out, aiming to disintegrate the cohesive structure by fluidisation of the cement powder with air before undertaking the powder stockage in silo. The fluidisation process of cohesive cement powder would lead to the suspension of the agglomerates (made up of primary particles) at a very high gas velocity (above the minimum velocity).

The cement powder is mainly composed of polymorphism Alite particles which could be assessed by a number of asperities in contact. These in turn will enhance the Van der Waals forces interaction, which is an interesting area of research that needs to be further, investigated.

References

Aïtcin PC, Jolicoeur C, MacGregor JG (1994) The reology of cementitious materials. *Concrete International*. 16(5): 45.

Boumiz A, Sorrentino D, Vernet C et al. (1997) Modelling the development of the elastic moduli as a function of the degree of hydration of cement pastes and mortars, in *Proceedings 13 of the 2nd RILEM Workshop on Hydration and Setting: Why does cement set? An interdisciplinary approach,* edited by A. Nonat (RILEM Dijon, France).

Castellanos A (2005) The relationship between attractive interparticle forces and bulk behaviour in dry and uncharged fine powders. *Advances in Physics*. 54 (4): .263-376.

Courtial M, de Noirfontaine MN, Dunstetter F et al. (2003) Polymorphism of tricalcium silicate in Portland cement : a fast visual identification of structure and superstructure. Powder Diffr. 18(1): 7-15.

Diederich P, Moureta M, Ryckc A et al. (2012) The nature of limestone filler and self-consolidating feasibility—Relationships between physical, chemical and mineralogical properties of fillers and the flow at different states, from powder to cement-based suspension. *Powder Technology*. 218: 90-101.

EN 197-1 (2011) Cement-Part 1: Composition, specifications and conformity criteria for common cements.

Flatt RJ (2004) Dispersion forces in cement suspensions. *Cement and Concrete Research*. 34(3) : 399-408.

Forsyth AJ, Hutton S, Rhodes MJ (2002) Effect of cohesive interparticle force on the flow characteristics of granular material. *Powder Technology*.126(2): 150-154.

Ganesan V, Rosentrater KA, Muthukumarappan K (2008) Flowability and handling characteristics of bulk solids and powders – a review with implications for DDGS. *Biosystems engineering*. 101(4): 425-435.

Geldart D (1973) Types of gas fluidization. *Powder Technology*. 7(5): 285- 292.

Götzinger M, Peukert W (2003) Dispersive forces of particle–surface interactions: direct AFM measurements and modeling. *Powder Technology*. 130 (1-3): 102-109.

Hamaker H C (1937) The London—van der Waals attraction between spherical particles. *Physica*.1937; 4 (10): 1058-1072.

Holdich R G (2002) Fundamentals of Particle Technology (ISBN: 9780954388102). Midland Information Technology and Publishing.

Johnson K L, Kendall K, Roberts AD (1971) Surface Energy and the Contact of Elastic Solids. Proceedings of the Royal Society A: Mathematical, Physical and Engineering 324(1558): 301-313.

Krupp H (1967) Particle Adhesion Theory and Experiment. *Advanced Colloidal Interface Science*: 111-239.

Langbein D (1969) Van Der Waals Attraction Between Macroscopic Bodies. *Journal of Adhesion.* 1 (4) : 237-245.

Leturia M, Benali M, Lagarde S et al. (2014) Characterization of flow properties of cohesive powders: A comparative study of traditional and new testing methods. *Powder Technology*. 253: 406-423.

Li LG, Kwan AKH (2014) Packing density of concrete mix under dry and wet conditions. *Powder Technology*. 253 (1): 514-521.

Li Q, Rudolph V, Peukert W (2006) London-van der Waals adhesiveness of rough particles . *Powder Technology*. 161(3): 248-255.

Lomboy G, Sundararajan S, Wang K et al. (2011) A test method for determining adhesion forces and Hamaker constants of cementitious materials using atomic force microscopy. *Cement and Concrete Research*. 41 (11): 1157-1166.

London F (1937) The general theory of molecular forces. Transactions of the Faraday Society. 33: 8b.

Maynard EP (2004) Practical solutions for solving bulk solids flow problems. Cement IndustryTechnical Conference, IEEE-IAS/PCA.

Molerus O (1973) Theory of yield of cohesive powders. *Powder Technology*. 12 (3): 259-275.

NA 442 (2005) Cement composition, specifications and conformity criteria for common cements.Edition number: 3. Algeria. See: http://www.ecde.dz/files/ft_ciment.pdf

Nakagaki M, Sunada H (1968) Theoretical studies on structures of sedimentation bed of spherical particles. Yakugaku Zasshi: 88-65.

Ramachandran VS, Malhotra VM, Jolicoeur C et al. (1998) Technical report, Ministry of public works and government services, Ottawa, Ontario, Canada . ISBN 0-660-17393-X.

Rumpf H (1962) in Agglomeration. W.A. Knepper (Ed.), Wiley: New York: 379.

Sauter J (1926) Die Grössenbestimmung der in Gemischnebeln von Verbrennungskraftmaschinen vorhandenen Brennstoffteilchen. German: VDI-Verlag G.M.B.H.

Schulze D (2008) Powders and Bulk Solids Behavior, Characterization,Storage and Flow, Springer-Verlag: Heidelberg: 35–74 ISBN 978-3-540-73768-1.

Schulze D (1995) Appropriate devices for the measurement of flow properties for silo design and quality control. 3rd Euro. Symp. Storage and flow of particulate solids, PARTEC, Nuremberg/ Germany. 21: 45-56.

Siegel S, Carr JW, Hanus EJ (1963) Polytetrafluorethylene Tipped Tablet Punches. *Journal of Pharmaceutical Sciences*. 52 (6): 604.

Tomas J (2007) Micromechanics of particle adhesion—an analytical approach. In: Eberhard, P. (Ed.), IUTAM Symposium on Multiscale Problems in Multibody System Contacts. Springer, Stuttgart: 301–316.

Turki D, Fatah N, Saidani M (2015) The impact of consolidation and interparticle forces on cohesive cement powder. *International Journal of Materials Research*. 106(12): 1258-1263.

Turki D, Fatah N (2010) Description of consolidation forces on nanometric powders. Brazilian Journal of Chemical Engineering. 27(4): 555-562.

Uchikawa H, Hanehara S, Sawaki D (1997) The role of steric repulsive force in the dispersion of cement particles in fresh paste prepared with organic admixture. *Cement and Concrete Research*. 27 (1): 37-50.

Xie HY (1997) The role of interparticle forces in the fluidization of fine particles. *Powder*

Technology. 94 (2): 99-108.

Figure 1

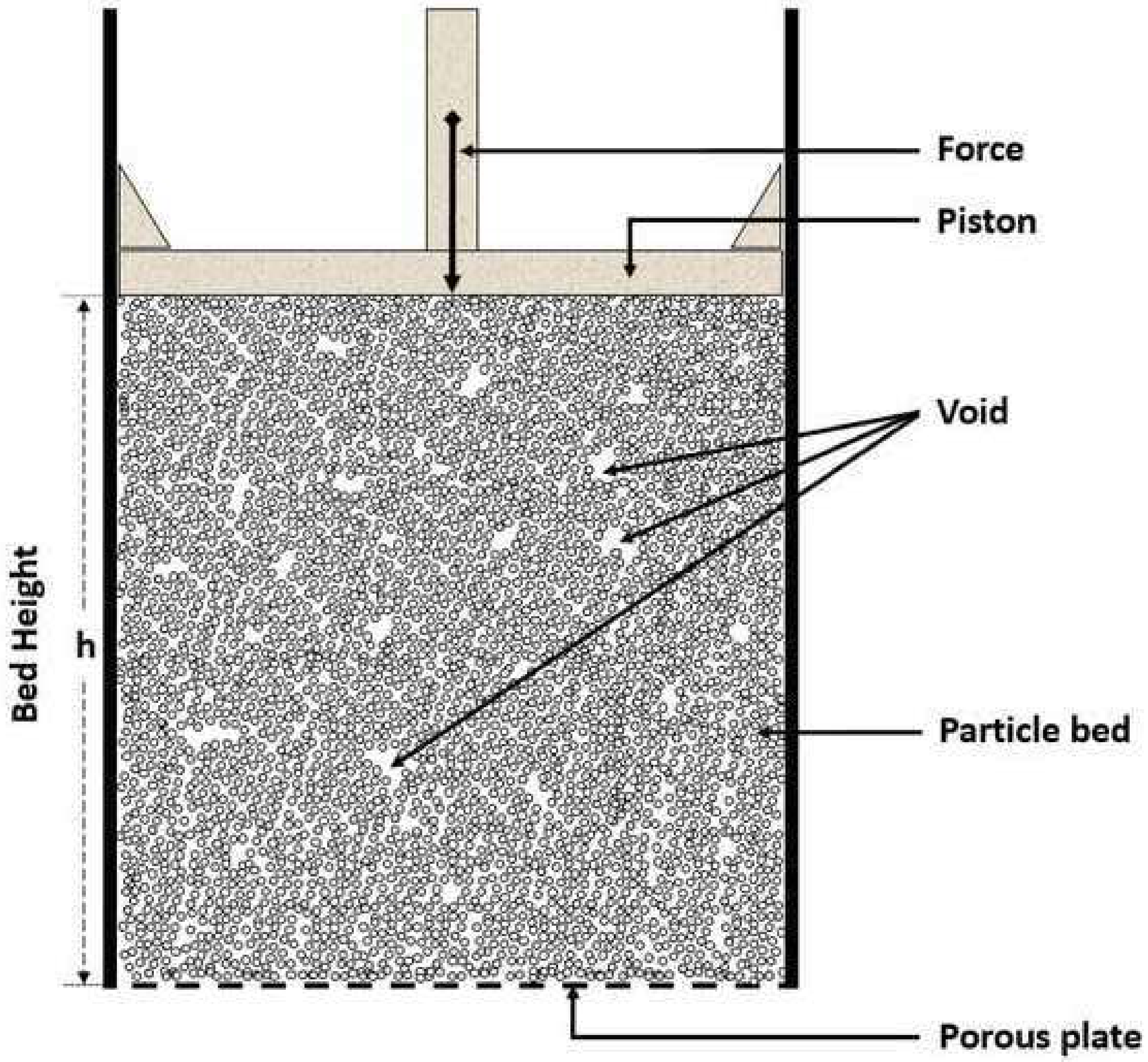

Figure 2

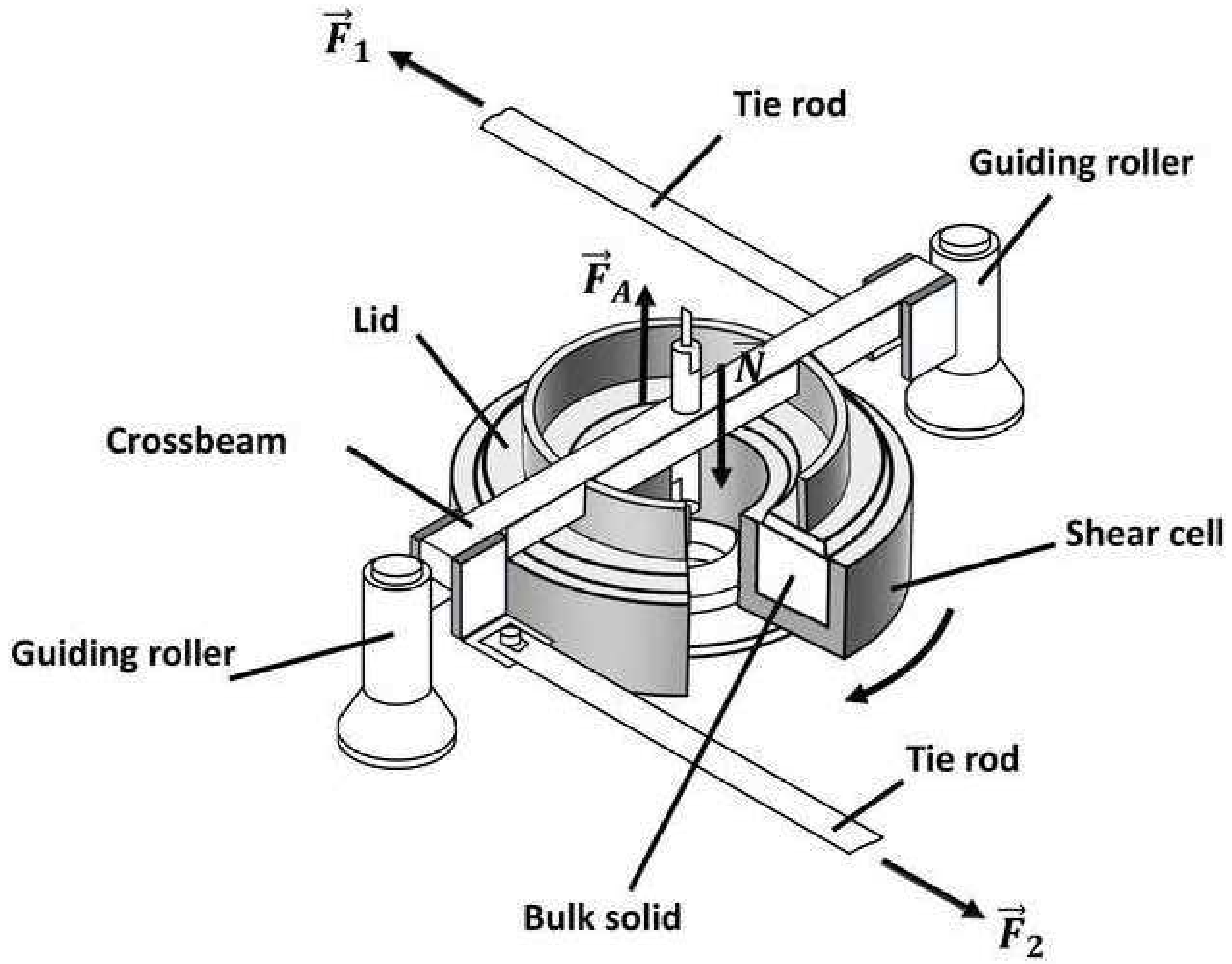
$\vec{F}_1$
Tie rod
Guiding roller
$\vec{F}_A$
Lid
$\vec{N}$
Crossbeam
Shear cell
Guiding roller
Tie rod
Bulk solid
$\vec{F}_2$

Figure 3

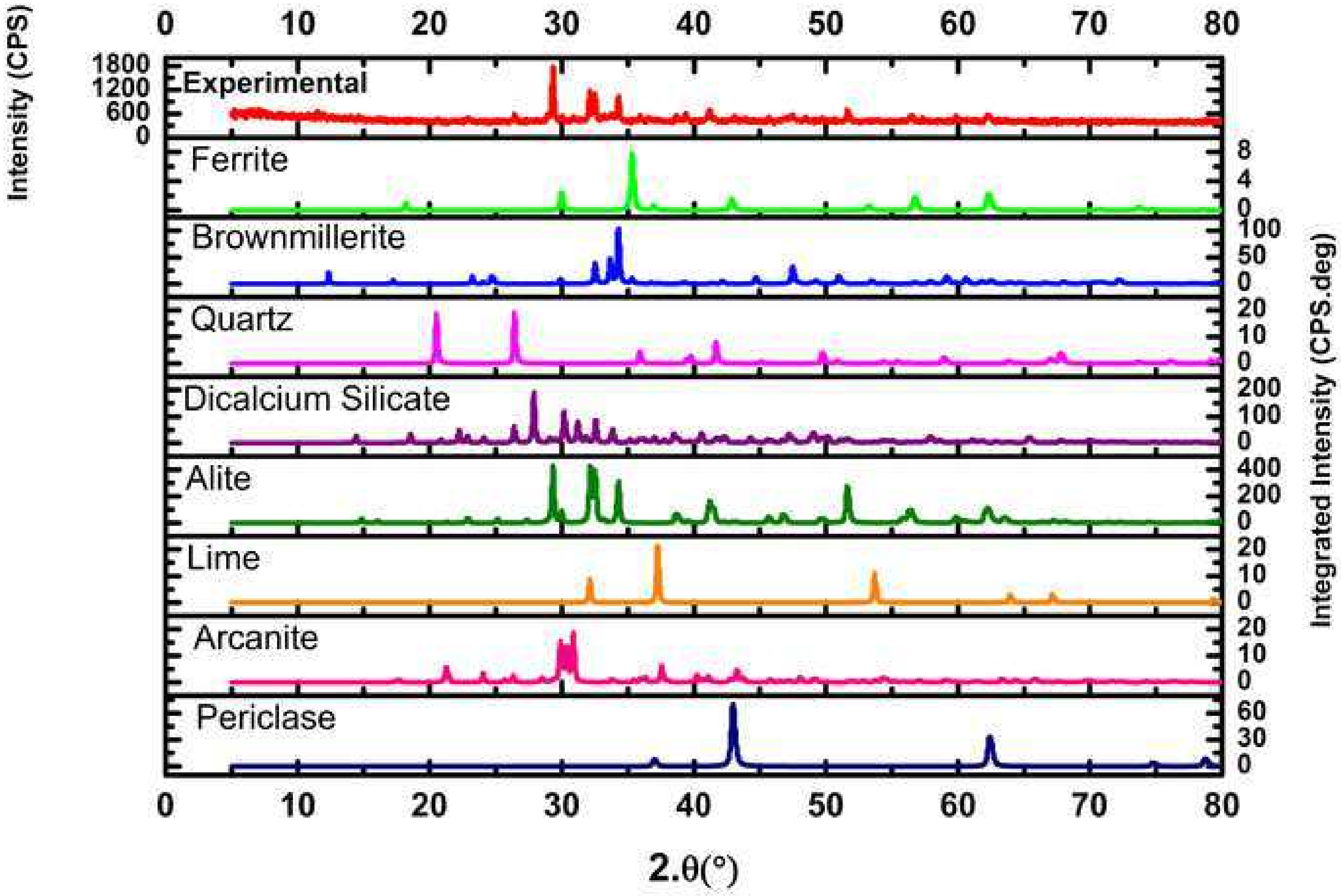
Intensity (CPS)
Integrated Intensity (CPS.deg)
Experimental
Ferrite
Brownmillerite
Quartz
Dicalcium Silicate
Alite
Lime
Arcanite
Periclase
2.θ(°)

Figure 4

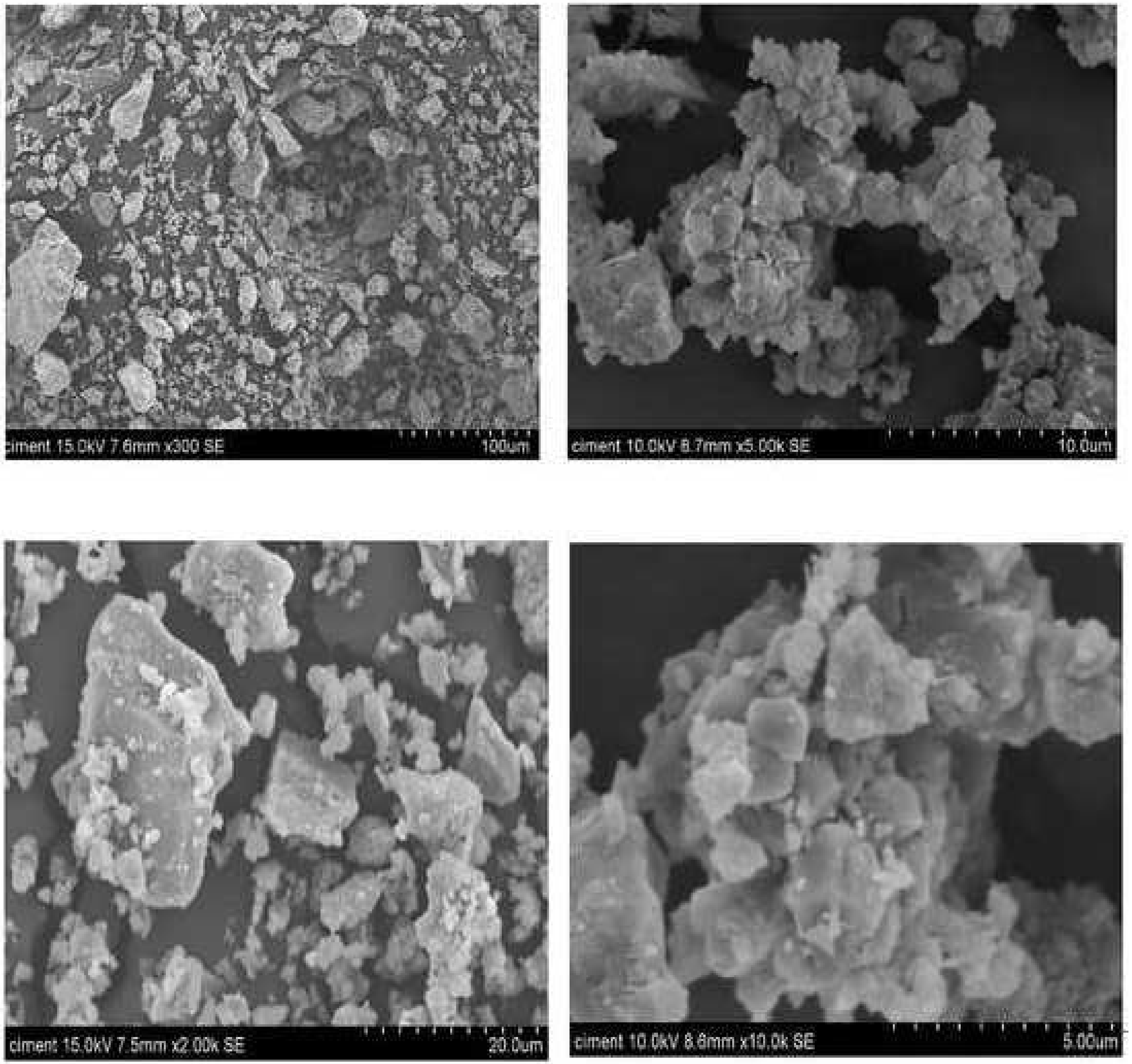

ciment 15.0kV 7.6mm x300 SE
100um
ciment 10.0kV 8.7mm x5.00k SE
10.0um
ciment 15.0kV 7.5mm x2.00k SE
20.0um
ciment 10.0kV 8.6mm x10.0k SE
5.00um

Figure 5

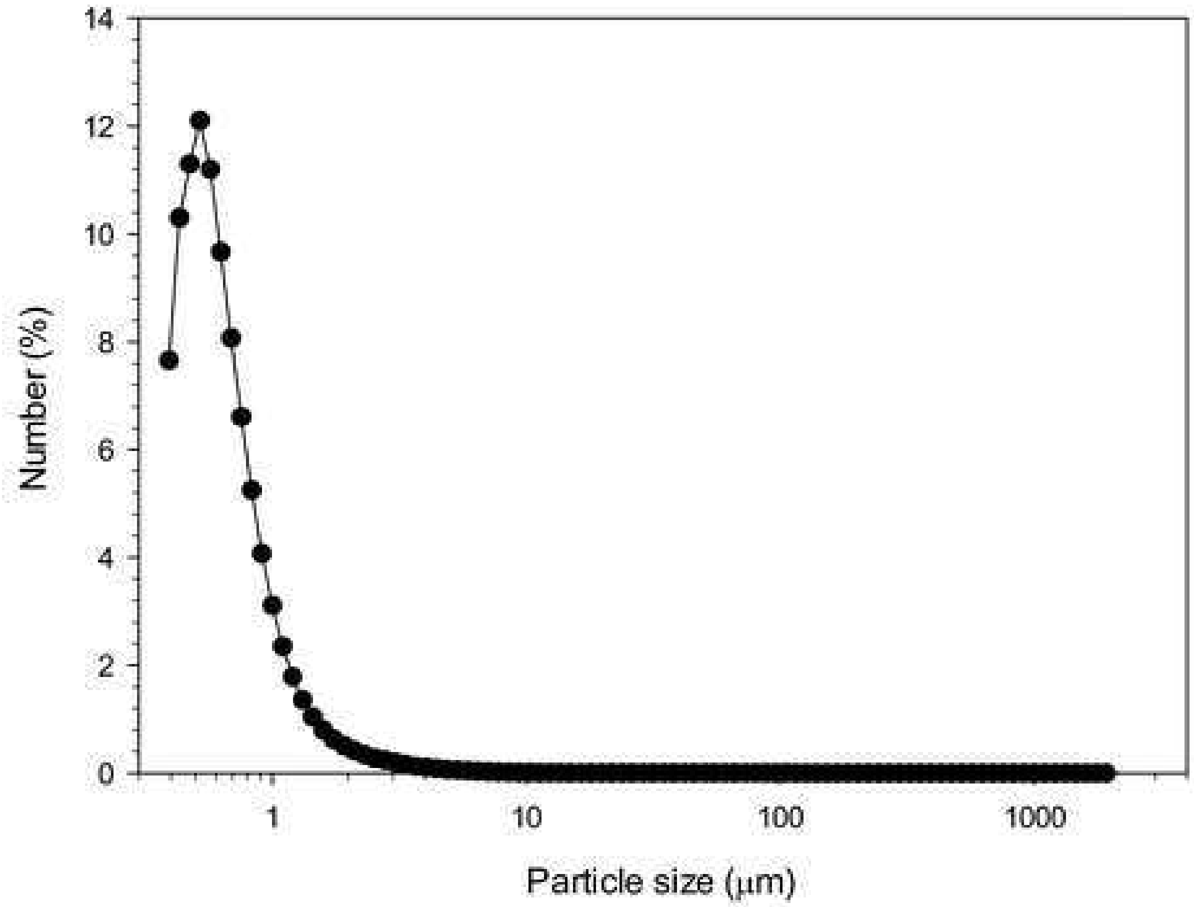

Figure 6

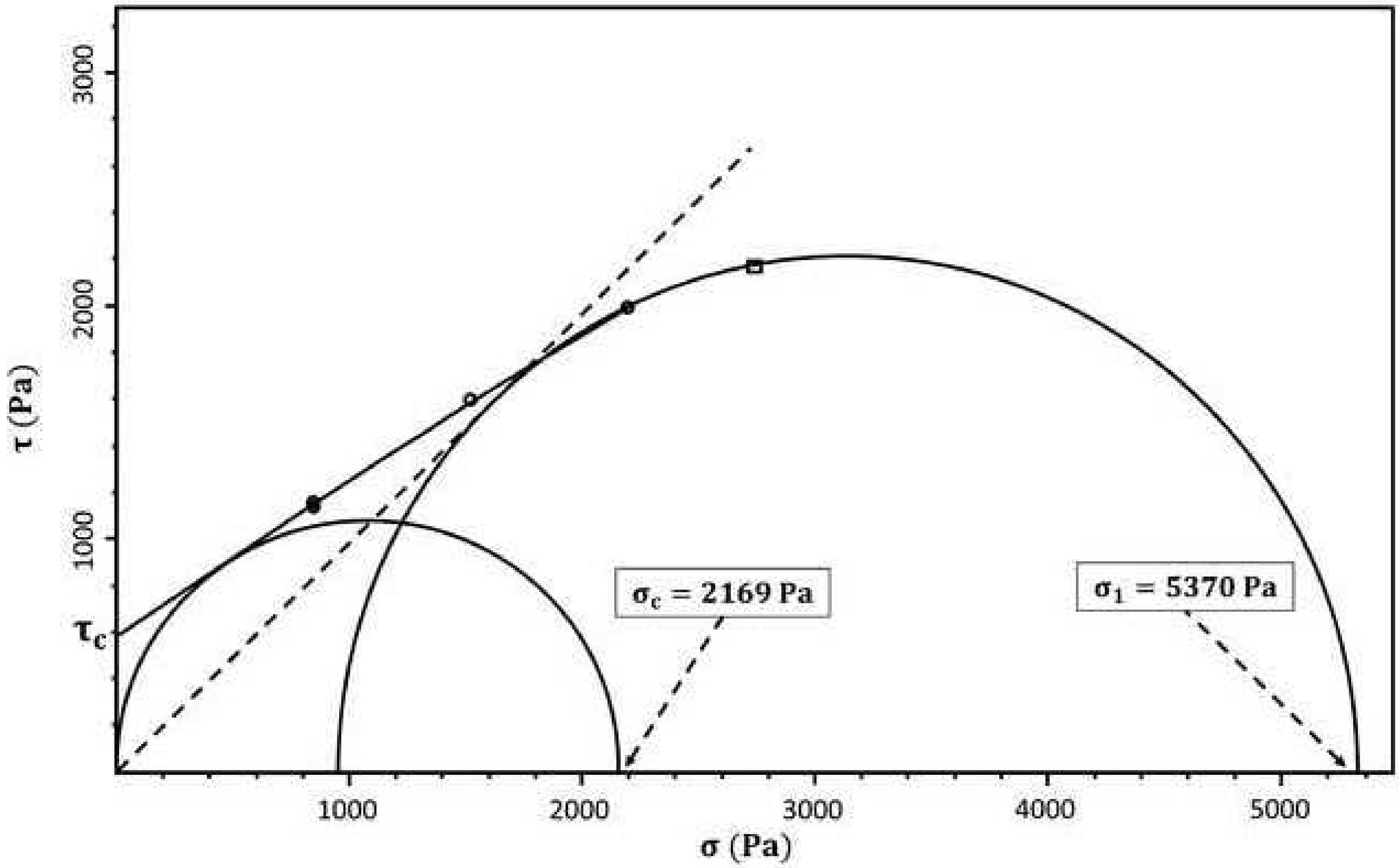

τ (Pa)
3000
2000
1000
τc
σc = 2169 Pa
σ1 = 5370 Pa
1000
2000
3000
4000
5000
σ (Pa)

Figure 7

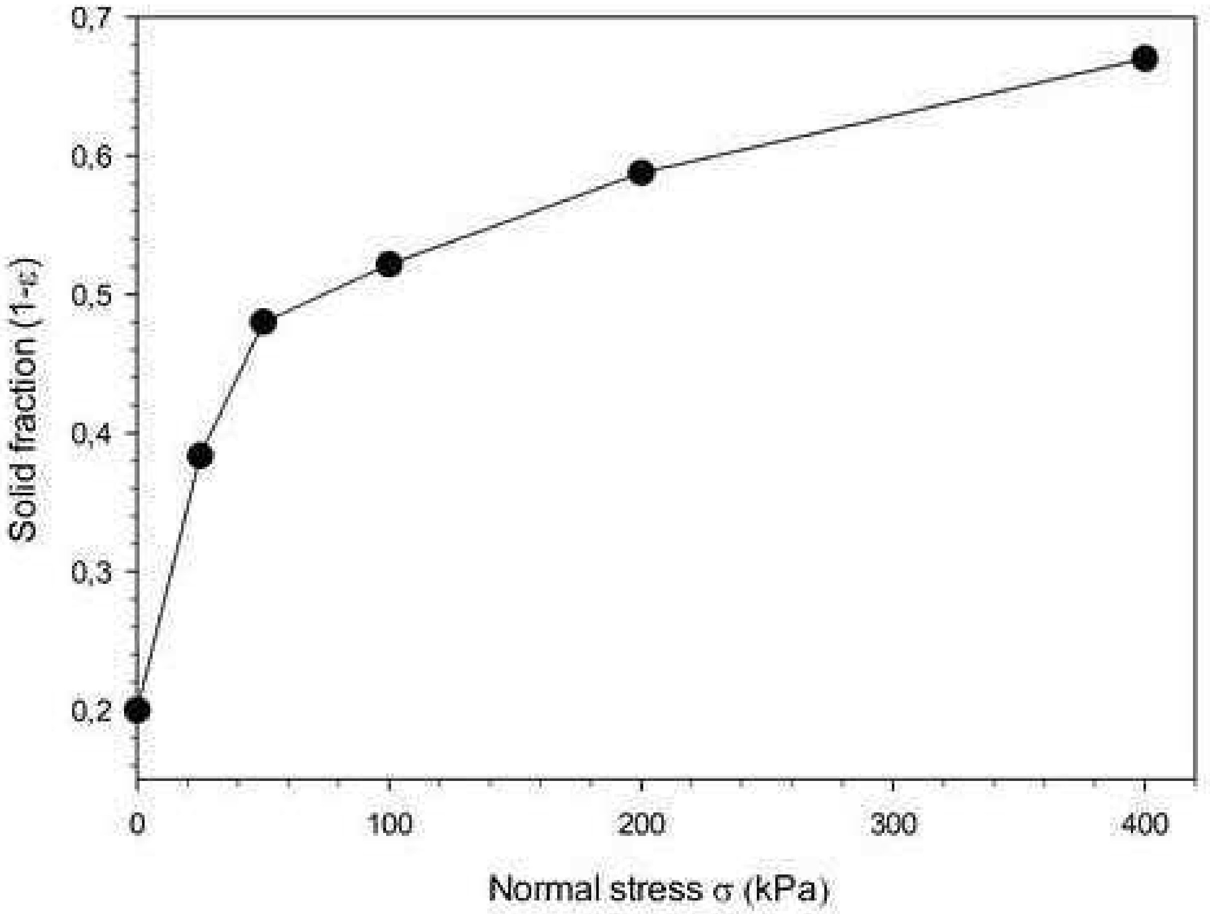

Solid fraction (1-ε)
0,7
0,6
0,5
0,4
0,3
0,2
0
100
200
300
400
Normal stress σ (kPa)

Figure 8

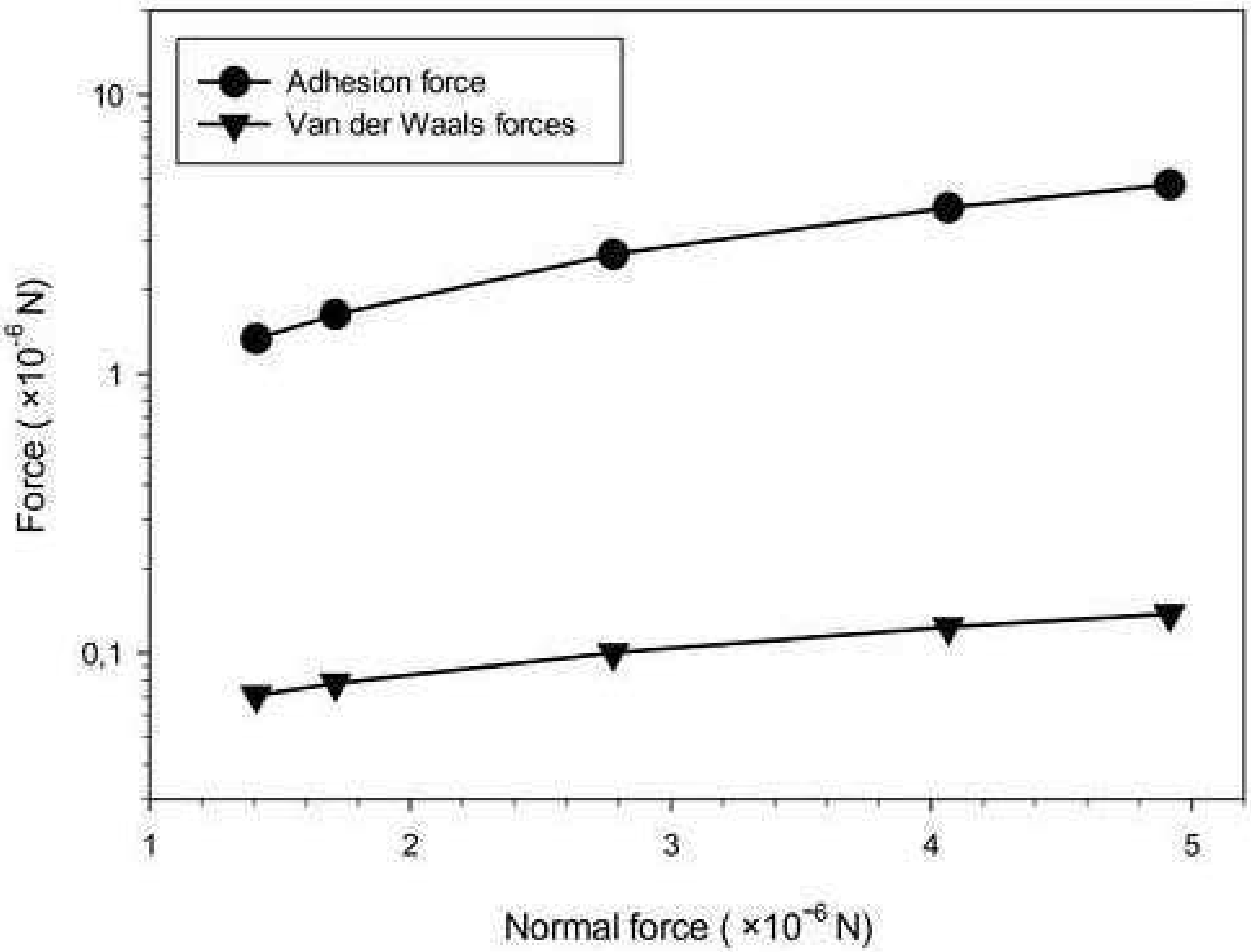
Adhesion force
Van der Waals forces
10
1
0,1
Force (×10-6 N)
1
2
3
4
5
Normal force (×10-6 N)

Figure 9

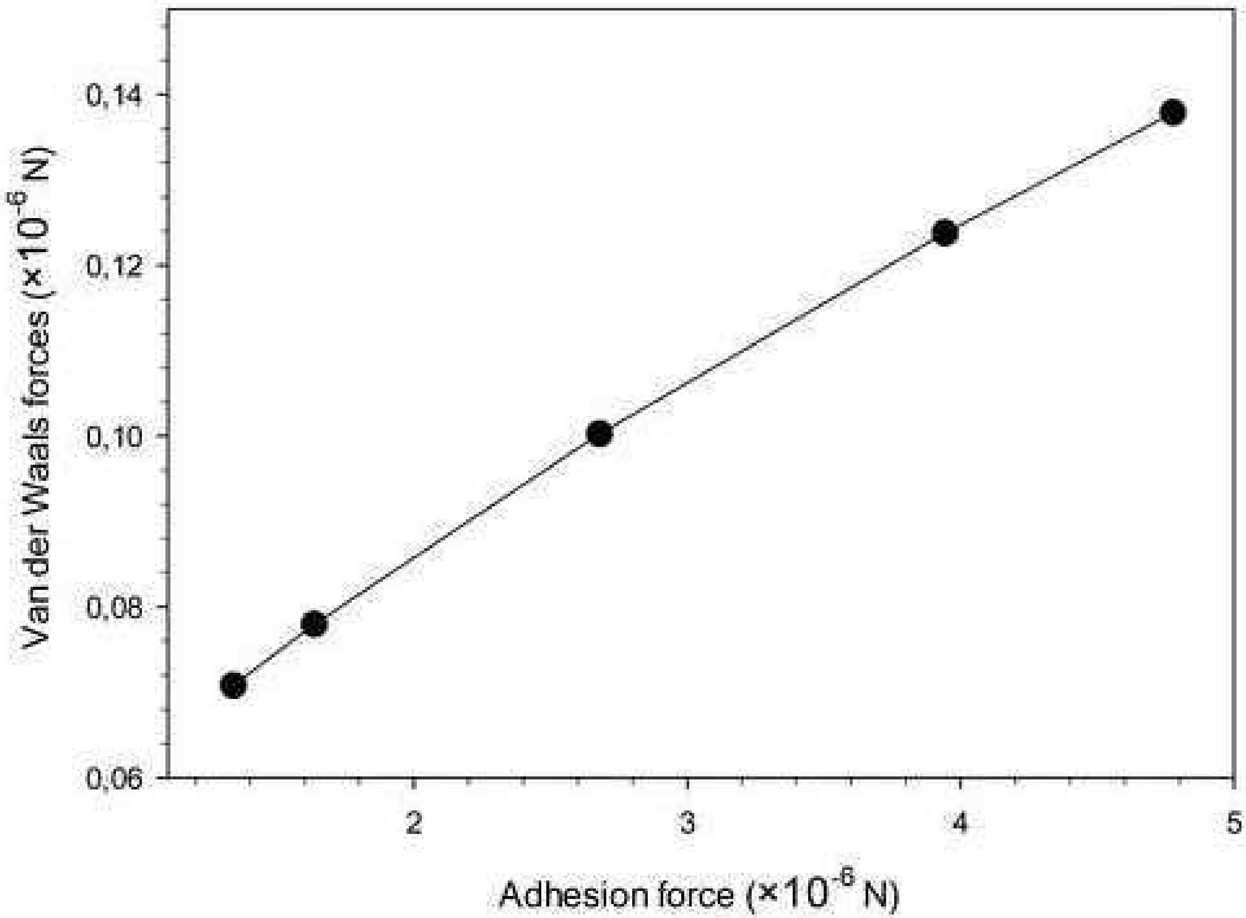
Van der Waals forces (×10-6 N)
0,14
0,12
0,10
0,08
0,06
2
3
4
5
Adhesion force (×10-6 N)

Figure 10

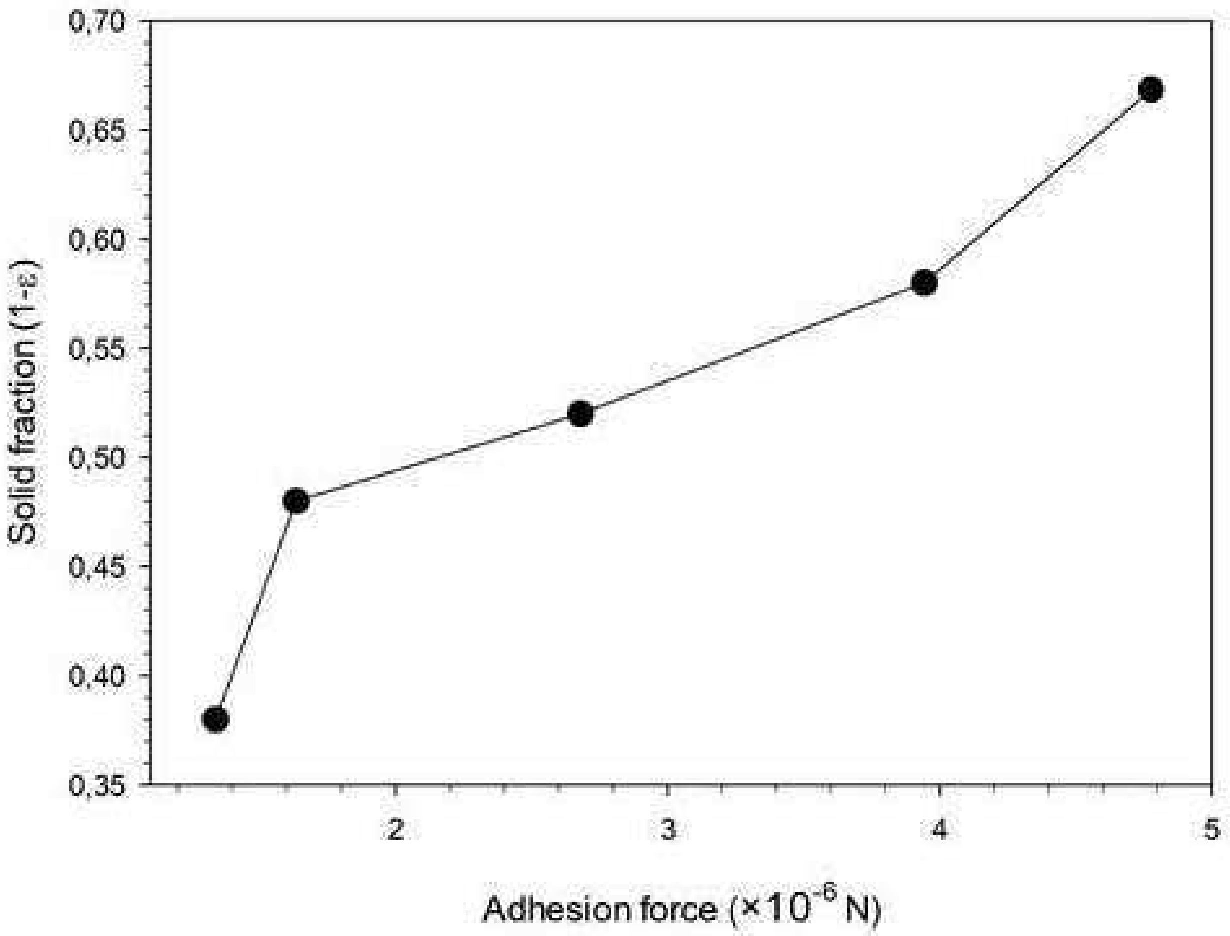
Solid fraction (1-ε)
0,70
0,65
0,60
0,55
0,50
0,45
0,40
0,35
2
3
4
5
Adhesion force (×10-6 N)

Table 1a

Chemical composition of cement CEM II/A-L 42.5 N		
Component	**Mean value (%)**	**Standard deviation**
Fe_2O_3	2.822578	0.068299
K_2O	0.782745	0.029200
MgO	0.814106	0.283107
S_iO_2	14.56387	0.432004
$Al_2\ O_3$	3.264997	0.148407
Na_2O	0.000394	0.002587
CaO	73.47939	0.473208
SO_3	3.902756	0.347077
T_iO_2	0.242009	0.013455

Table 1b

Physical and mechanical properties of cement CEM II/A-L 42.5 N		
Initial setting time (min)	125	
Final setting time (min)	185	
Thermal expansion (mm)	0.47	
Specific area (Blaine) (cm^2/g)	4465	
Standard consistency (%H_2O)	27.04	
	Compressive strength (MPa)	**Flexural strength (MPa)**
2 days	23.19	4.99
7 days	35.24	6.78
28 days	44.64	7.80

Table 2

Phase name	Content (%)
Alite	51
Brownmillerite	15
Periclase	11.7
Ferrite	9.2
Quartz	5.4
Belite (Dicalcium Silicate)	4.7
Portlandite	1
Arcanite	1
Lime	0.8

Table 1a. Micro-XRay Fluorescence spectrometer analysis of the cement class CEM II/A-L 42.5 N

Table 1b. Physical characteristics of cement class CEM II/A-L 42.5 N conforming to NA442 (or EN 197-1:2011) See:(https://www.scimat.dz/portail/gamme/ciments/)

Figure 1. Consolidation test

Figure 2. Annular shear cell Schulze (1995)

Figure 3. Diffraction patterns of Portland cement (OPC) of class CEM II/A-L 42.5 N

Table 2. Quantitative analysis of Portland cement (OPC) of class CEM II/A-L 42.5 N

Figure 4. SEM photos of cement (OPC) of class CEM II/A-L 42.5 N, scaling (100 μm, 20 μm, 10 μm and 5μm)

Figure 5. Particle size distribution of cement powder

Figure 6. The Mohr's circle and yield locus of cement powder Turki et al. (2015)

Figure 7. Variation in solid fraction according to the normal stress for cement powder Turki et al. (2015)

Figure 8. Variation of the adhesion and Van der Waals forces vs. the normal force

Figure 9. The variation of Van der Waals forces to the adhesion force

Figure 10. The evolution of the solid fraction according to the adhesion force